SI Appendix 1

1. Additional Methods

Measures of cell density. The cell density is determined in two independent ways by measurement of the optical density at 620 nm (OD) and the dry weight (dw) of the cells. Fig. 6 illustrates the linear relation between OD and the total dry weight $\mathrm{dw_T}$ which is the sum of the dry weight of the cells, dw, and the dry weight of the buffer.

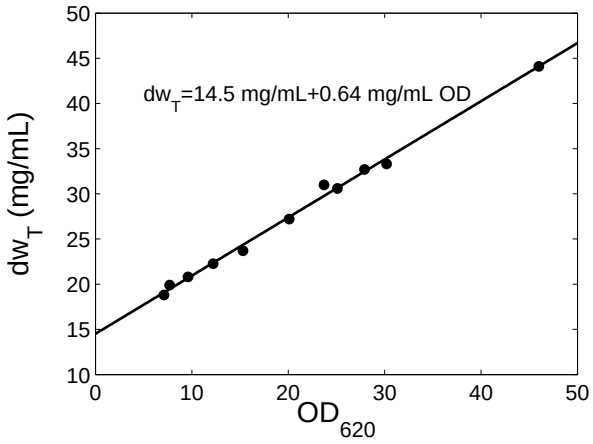

Fig. 6. Linear relation between OD and total dry weight $\mathrm{dw_T}$. The regression line is used to assign confidence intervals to the cell density measurements in Figs. 2, 3 and 12.

The volume ratio $\alpha = V_{\mathrm{cyt}}/V_{\mathrm{x}}$ is proportional, in the range of α values we consider, to OD and dw according to $\alpha = 0.0014$ OD $= 0.0022$ ml per mg of dw (ref. 1 and our wet weight measurements).

Data analysis and determination of dynamical properties. The properties of the collective dynamics (amplitude and frequency of the oscillations, rate of decay to the equilibrium) are determined by processing the NAD(P)H fluorescence time series in order to obtain a smooth oscillatory signal with defined amplitude and phase.

Autonomous oscillations. For the cell densities at which spontaneous oscillations occur, the fluorescense signal is processed according to the following steps:

1. The baseline (Fig. 7) is computed by using a running average with a time window corresponding to two periods of oscillations.

2. An initial transient is discarded. It appears as an exponential decay of the baseline to a steady state, and its duration is of the order of one hour.

3. To compare signals from measurements at different cell densities, the signal is normalized by subtracting the baseline and dividing by the baseline value. By using the Hilbert Transform (2) on trains of ten to fifty periods we obtain for each datapoint the instantaneous amplitude (Fig. 8) and phase (Fig. 9) of the corresponding regular oscillator generating the observed signal.

4. *Amplitude* A is obtained by averaging the instantaneous, normalised amplitudes within each train. The angular *frequency* ω is calculated as the mean slope of the phase time series (Fig. 9). The

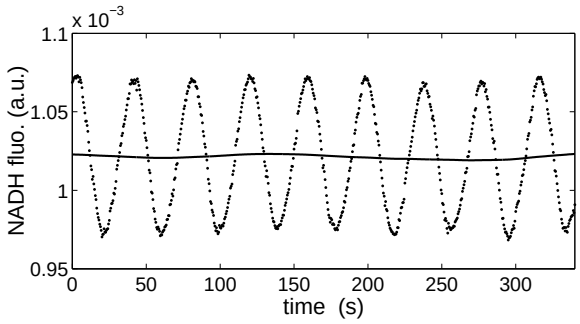

Fig. 7. Experimentally measured fluorescence time trace at a cell density of dw=11 mg/ml, above the critical cell density. Each dot corresponds to one measurement (time interval between two measures $\Delta t = 0.5$ s). The continuous line represents the baseline.

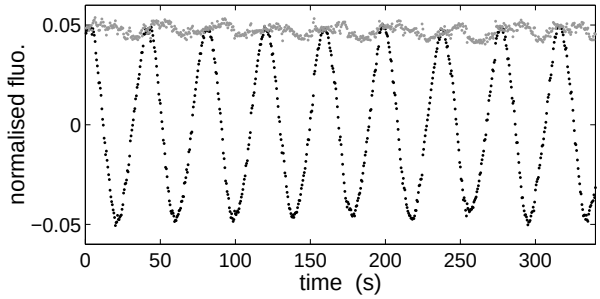

Fig. 8. Normalised time series of Fig. 7 (black dots) and the instantaneous amplitude computed from the Hilbert transform (gray dots).

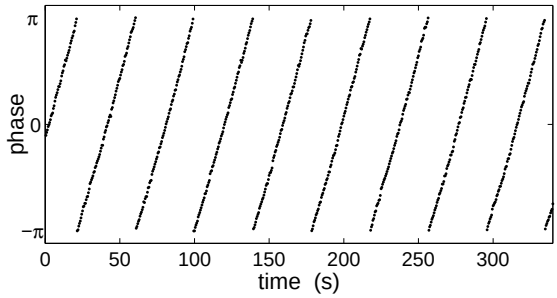

Fig. 9. Instantaneous phase of the signal in Fig. 7 computed from the Hilbert transform.

frequencies measured soon after the exhaustion of the transient and at the end of the experiment are used as a check against possible drift of the operating point.

5. Amplitude and frequency are computed for about five non-overlapping time windows. Figs. 2 and 3 display their averages with error bars indicating the maximum and minimum values.

Macroscopic steady state. When the signal is not oscillating, the dynamical properties of the system cannot be determined without perturbation experiments. In this study, we force the solution with a periodic inflow of Aca with a period of 39 seconds, close to that of the damped oscillations of the unforced system. For half of the period, the Aca inflow is set to twice its unforced rate, for the other half period it is stopped, thus maintaining the same average inflow over a period as in the unforced system. This results in an approximately saw-tooth shaped variation of the mixed flow Aca concentration, which forces the system to oscillate at a fixed amplitude (Fig. 10, grey dots). After such a forcing is stopped, the collective dynamics decays back to the steady state (Fig. 10, black dots). The signal is processed as

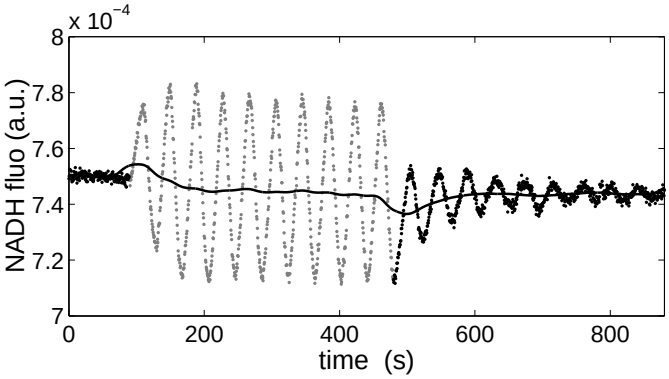

Fig. 10. NAD(P)H fluorescence signal before, during and after forcing of a non spontaneously oscillating suspension (dw=4.1 mg/ml, below the critical density). In the absence of external forcing (black points) the average fluorescence of the steady state is constant up to the experimental precision (0.5%). When forced with a period of 39 s (grey dots) the cells respond immediately and synchronize with the external signal. When forcing is terminated, the fluorescence displays a damped decay. The black line shows the baseline used for data cleaning and processing. The average Aca inflow is the same throughout the experiment.

for points 1 – 3 of the spontaneous oscillating case. However, the frequency ω is computed only on the decaying regime and after the baseline has recovered from the small drift of the operating point (due to the local change of Aca). The exponential fit of the amplitude decay (Fig. 11, *Inset*) yields λ.

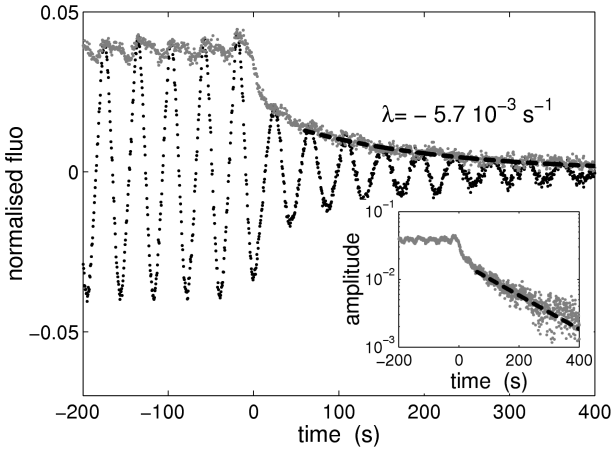

Fig. 11. Experimental data shown in Fig. 10 after subtraction of the baseline and normalisation (black dots) and the relative amplitude computed from the Hilbert transform (grey dots). The dashed line represents an exponential decay towards the origin with exponent λ and is displayed in a semilog plot in the inset. The amplitude has a first abrupt decay (similar for all the experimental conditions we have explored) that we explain as a displacement of the limit cycle, due to the forcing, out of the plane of natural oscillations. This is followed by an exponential decay up to the point where noise levels the signal off. Time $t = 0$ s corresponds to the interruption of the forcing.

These two quantities correspond to the imaginary part ω (Fig. 2, filled circles) and real part λ (Fig. 12) of the complex Hopf eigenvalues of the Jacobian matrix for the collective dynamics in the stable steady state. Figs. 2 and 12 display the average value of about five repetitions of the perturbation protocol. The error bars correspond to the maximum and minimum observed values. For very dilute suspensions, the measurement of these exponents is hampered by the increasingly fast damping as the cell density decreases. This reduces the time interval over which statistics can be performed. We did not consider density values for which the signal had less than five clearly distinguishable damped oscillations.

Data fit and parameter estimation. The parameters of the reduced equation (Eq. **2**) are determined by sequential fitting of Eqs. **3 – 5** to the experimental data (Figs. 2 – 3 and 12). First, the density is expressed in terms of α as described in the *Measures of the cell density*. A fit of Eq. **3** to the frequency data (Fig. 2) determines c and ω_0 ($c = 850$, $\omega_0 = 0.17\ \mathrm{s}^{-1}$). These parameter values can be inserted in Eq. **4**, and the remaining parameters of this equation (τ and λ_0) are determined by fitting to the linear stability data (Fig. 12).

This yields $\tau = 0.16\ \mathrm{s}^{-1}$, $\lambda_0 = 0.015\ \mathrm{s}^{-1}$ and a critical cell density of $\mathrm{dw}^* = 5.6$ mg/ml. We are now left with only one free parameter, the nonlinearity coefficient g. Eq. **5** can, in turn, be used to fit the amplitude data (Fig. 3). By substituting the previously fitted parameters, we can obtain two independent values for the nonlinearity parameter g ($g = -3.6\ \mathrm{s}^{-1}$ or $g = -4.0\ \mathrm{s}^{-1}$, within 12% from each other). Alternatively, if we only introduce λ_0 in Eq. **5**, we get an independent estimate of the critical cell density $\mathrm{dw}^* = 6.3$ mg/ml, which is within 13% from the value obtained by fitting the first two equations. The closeness of these estimates confirms the self-consistency of the model in explaining the experimental data.

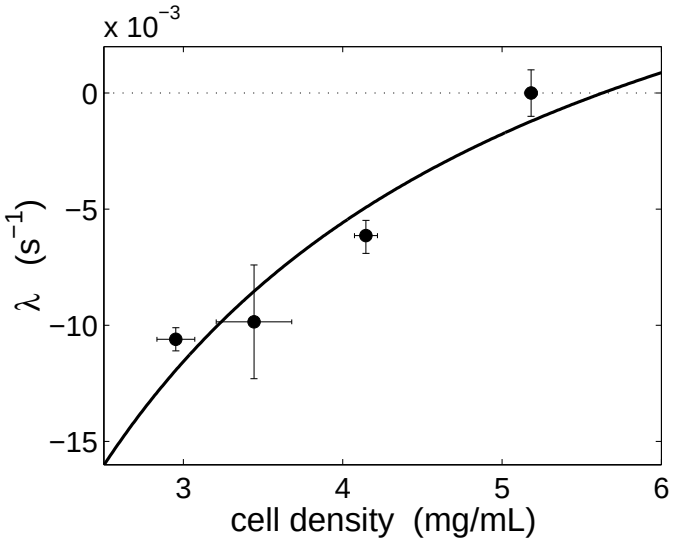

Fig. 12. Decay exponent (real part of the complex eigenvalues of the stable steady state; dots) as a function of cell density (reported as dry weight). The continuous line represents the best fit of Eq. **4**.

Besides the parameters obtained by means of the reduced equation, the full system Eq. **1** depends on additional parameters that cannot be directly inferred from the scaling relations. These parameters have to be specified in the comparison of the experimental data with the numerical simulations, where the intracellular oscillator is embedded into a three-dimensional chemical space (see *Mathematical Model*).

The angle $\theta = 87^\circ$ between the oscillation plane and the direction of the diffusing species has a complex relation with the parameters of the reduced system. We choose its value so that the rescaling parameter c of the simulations matches that of the reduced system.

The rate of decay to the oscillations plane and the diffusion constant are chosen large but finite, consitent with our hypothesis of large time scale separation of the oscillatory modes and of fast diffusion. The values we use in the numerical simulations are: $-\lambda_{\mathrm{fast}} = 500\ \mathrm{s}^{-1}$ and $d_{\mathrm{aca}} = 300\ \mathrm{s}^{-1}$ (cf. Section 2). The larger their values, the better the reduced system approximates Eq. **1**.

For simulations of populations of non-identical oscillators, we also need to choose the features of the frequency distribution. We assign the frequencies ω_j of each of the oscillators according to a Gaussian distribution centred in ω_0. The relative standard deviation of this distribution is 15%; this is a larger range of frequency variation than we observe experimentally in the bulk oscillations.

2. Estimate of Acetaldehyde Transport Kinetics

Acetaldehyde (Aca) is a small uncharged molecule that diffuses freely across the cell membrane. It is believed to be the mediator of the diffusive coupling among the yeast cells (3). The strength of the coupling is hence proportional to the first-order rate constant d_{aca}, which quantifies the kinetics of the Aca transport reaction.

In order to enter the yeast cell, an Aca molecule has to cross first an unstirred boundary layer surrounding the cell, and then the cell membrane. Based on diffusion equations (4), we can give an estimate of d_{aca}.

We take the yeast cell as a sphere of radius r_1, and the boundary layer as a spherical shell of inner radius r_1 and outer radius r_2. In doing this, we consider that the cell membrane (of the order of 10 nm) has a negligible thickness compared to the boundary layer. The diffusion flux is most readily estimated under the assumption of a quasi-stationary concentration profile. With this assumption, the amount of diffusing substance passing the cell membrane per unit time is given by ref. 4 (p. 84):

$$J = \frac{4\pi D}{\frac{1}{r_1} - \frac{1}{r_2}}(c_2 - c_1),$$

where J is the flux of particles (molecules per unit area per time), D is the diffusion coefficient (unit area per unit time) and c_i is the concentration at $r = r_i$. Expressed in terms of intracellular concentration, this is equivalent to:

$$\frac{J}{V_1} = 3\,D\,\frac{c_2 - c_1}{r_1^2 - \frac{r_1^3}{r_2}} = d_{\mathrm{aca}}\,(c_2 - c_1),$$

where V_1 designates the volume of a sphere of radius $r = r_1$.

In order to estimate d_{aca} we take $r_1 = 3\ \mu\mathrm{m}$, which is the radius of a sphere with the same volume as a typical yeast cell. We also take $r_2 = 6.5\ \mu\mathrm{m}$ which is the largest geometrically possible boundary layer which can be accomodated at the typical cell density of 10% wet weight. Finally, we take $D = 5 \cdot 10^{-6}\ \mathrm{cm}^2/\mathrm{s}$ which is a typical small-molecule diffusion coefficient. With these values one obtains

$$d_{\mathrm{aca}} = \frac{3\,D}{r_1^2 - \frac{r_1^3}{r_2}} = 300\ \mathrm{s}^{-1}.$$

The validity of the assumption of quasi stationarity of the concentration profile can be assesed by means of the time-dependent diffusion equation. From ref. 4 (p. 95) we get the smallest relaxation rate

$$k_{\mathrm{relax}} = \frac{D\pi^2}{(r_2 - r_1)^2} = 400\ \mathrm{s}^{-1}.$$

Both numbers are large compared to the timescales of the oscillatory intracellular dynamics, whose period is about 37 s and eigenvalue corresponding to the linear instability typically $0.015\ \mathrm{s}^{-1}$. Based on this result, we assume that the equilibration of Aca concentrations inside and outside the cell is almost instantaneous.

3. The Mathematical Model

Eq. **1** in the main text describes a population of oscillators diffusively coupled to a homogeneous external medium. Depending on parameter values, this system can display a number of dynamical regimes, which can be studied both at the individual and at the population level. Our interest for modelling at the population level comes from practical difficulties of measuring the state of the individual cells in a stirred reactor.

As pointed out in the main text, our experiments do not provide any indications in favour of an incoherent regime, and in particular they do not satisfy some of the hallmarks of the universal transition to coherence described by Kuramoto (5). We focus on the other scenario (i.e. synchronous collective

motion), which is consistent with the available experimental data on oscillating suspensions. Within this framework, and based on the assumption of a separation of time scales, we formulate a reduced equation describing the overall reactor dynamics, and from that we obtain scaling laws for the macroscopic observables. These equations allow us to parameterise the model by fitting it to the experimental data. Eventually, we will check the robustness of the quantitative model after relaxing the assumptions introduced for deriving the reduced equation. In particular, we will show the self-consistency of the synchrony hypothesis.

Reduced equation for the synchronous dynamics. With the aim of deriving a simple reduced equation accounting for the macrosopic bifurcation, we assume now that all cells are identical and that the diffusion through the membrane is much faster than the time scale of the intracellular dynamics. In the synchronous regime, the population described by Eq. **1** behaves as one single oscillator coupled to an external medium:

$$\begin{aligned} \frac{\mathrm{d}\mathbf{x}}{\mathrm{d}t} &= \mathbf{F}(\mathbf{x}) - \mathbf{D}(\mathbf{x}-\mathbf{X}) \\ \frac{\mathrm{d}\mathbf{X}}{\mathrm{d}t} &= \alpha\,\mathbf{D}\,(\mathbf{x}-\mathbf{X}) - \mathbf{J}\mathbf{X}. \end{aligned} \qquad \textbf{(S1)}$$

The dynamics of the overall concentrations is obtained by a sum of the two equations in Eq. **S1**, weighted by the relative volumes occupied by the cytoplasms V_{cyt} and by the medium V_{x}:

$$V_{\mathrm{cyt}}\frac{\mathrm{d}\mathbf{x}}{\mathrm{d}t} + V_{\mathrm{ext}}\frac{\mathrm{d}\mathbf{X}}{\mathrm{d}t} = V_{\mathrm{cyt}}\,\mathbf{F}(\mathbf{x}) - V_{\mathrm{cyt}}\,\mathbf{D}\,(\mathbf{x}-\mathbf{X}) + V_{\mathrm{ext}}\,\alpha\,\mathbf{D}(\mathbf{x}-\mathbf{X}) - V_{\mathrm{ext}}\,\mathbf{J}\,\mathbf{X}. \qquad \textbf{(S2)}$$

From the definition of $\alpha = V_{\mathrm{cyt}}/V_{\mathrm{x}}$, and if all substances cross the membrane very fast (so that we can set $\mathbf{x} \sim \mathbf{X}$), we get:

$$\frac{\mathrm{d}\mathbf{x}}{\mathrm{d}t} = \frac{\alpha}{\alpha+1}\,\mathbf{F}(\mathbf{x}) - \frac{1}{\alpha+1}\,\mathbf{J}\,\mathbf{x}. \qquad \textbf{(S3)}$$

This equation already contains in a nutshell the qualitative effects of a cell density change on the synchronous dynamics of a population. In the limit of infinite α (tightly packed cells), the macroscopic dynamics is identical to the intracellular dynamics $\mathbf{F}(\mathbf{x})$. If α is small, that is for very dilute suspensions, the extracellular relaxation dynamics $-\mathbf{J}\mathbf{x}$ prevails and $\mathbf{x} = \mathbf{0}$ is a stable solution. The transition from high to low cell densities takes place by a progressive slowing (due to the coefficient of the first term multiplying the intracellular dynamics) and damping of the dynamics.

Geometrical arguments suggest to apply Eq. **S3** also to cases where not all the species diffuse, through a rescaling of alpha. Such rescaling provides an effective cytosolic volume larger than the real one and thus reduces the effect of the extracellular medium. Specifically, numerical simulations show that a rescaled version of Eq. **S3** describes the overall reactor dynamics for the case of yeast, where planar oscillators are coupled by a fast diffusing species. The rescaling factor c depends on the geometrical relationships between the plane of oscillations and the direction along which the diffusive coupling takes place. The validity of the rescaling is confirmed, as discussed below, also if there is no complete separation of the time scales and for nonidentical oscillators.

Model of the intracellular oscillator. In accordance with experimental observations (6,7), we describe the dynamics of the individual yeast cell oscillator as a limit-cycle close to the onset of oscillations. Thus, the intracellular dynamics is modelled as a Hopf oscillator confined to a plane in concentration space, which is tangential to the unstable manifold of the stationary state. For the sake of simplicity, we assume that the average concentration of intracellular species is not affected by cell density, and center the limit cycle at the origin. In the plane of oscillations, the intracellular dynamics is described by a Hopf normal form (8):

$$\frac{\mathrm{d}z}{\mathrm{d}t} = f(z) = \left(\lambda_0 + i\omega_0 + g\,|z|^2\right) z, \qquad \textbf{(S4)}$$

where z is a complex variable, and $\lambda_0 \pm i\omega_0$ are the eigenvalues associated with the eigenvectors spanning the plane of oscillations. In the most general formulation, the nonlinearity parameter g is complex, and

its imaginary part makes the frequency of the free-running oscillator depend on the amplitude. Previous estimates of this parameter (7) have evidenced the small relative value of the imaginary part of g ($\frac{|\mathrm{Im}(g)|}{|\mathrm{Re}(g)|} = 0.2$) and we have observed no frequency shift in transients after forcing. Therefore, we here assume that g is real-valued.

The plane of oscillations is embedded in a high-dimensional concentration space. Close to the onset of oscillations, however, the dynamics is essentially confined to this plane. This corresponds to a sharp time scale separation between the oscillations and the fast transverse modes. The coupling acts along the direction(s) of the diffusing species, and these directions do generally not coincide with the plane of oscillations. This is the cause of the density rescaling introduced above.

In the case of yeast, Aca is known to diffuse extremely fast. When the description of the yeast glycolytic oscillations, Eq. **S4**, is substituted into Eq. **2**, this takes the form:

$$\frac{\mathrm{d}z}{\mathrm{d}t} = \frac{\alpha c}{\alpha c + 1}\left(\lambda_0 + i\omega_0 + g\,|z|^2\right) z - \frac{1}{\alpha c + 1}\tau z. \qquad \textbf{(S5)}$$

Separation of the radial and angular parts of this equation ($z = Re^{i\phi}$) yields:

$$\begin{aligned} \frac{\mathrm{d}R}{\mathrm{d}t} &= \frac{\alpha c}{\alpha c+1}\left(\lambda_0 + g\,R^2\right) R - \frac{\tau}{\alpha c+1} R \\ \frac{\mathrm{d}\phi}{\mathrm{d}t} &= \frac{\alpha c}{\alpha c+1}\,\omega_0. \end{aligned} \qquad \textbf{(S6)}$$

From these equations, we obtain the scaling laws Eqs. **3 – 5**. These scaling laws allow us to parameterise the reduced system by fitting the parameters ω_0, λ_0, c, τ and g to the experimental data, as described in Section 1.

4. Comparison of Fitted Parameters with Independent Estimates

Estimate of the linear stability of the intracellular steady state λ_0**.** We have previously determined the linear stability of the steady state by fitting the Hopf normal form with an additional stable mode to quenching experiments where the glycolytic oscillations are perturbed by addition of a single pulse of either Aca or glucose (7). This analysis indicates that $\lambda = 0.014\ \mathrm{s}^{-1}$ at a cell density of dw =16 mg/ml. This is in good agreement with the value of $\lambda_0 = 0.015\ \mathrm{s}^{-1}$ determined here.

Estimate of the relaxation time τ**.** An independent estimate of the first-order rate constant for extracellular removal of Aca can be obtained from biochemical data in the literature and the flow parameters of the reactor. The estimate is based on the observation that the balance of the chemical species present in the extracellular medium is due to three factors: (*i*) the flow through the reactor, entirely determined by its volume and by the rate at which chemicals are introduced, (*ii*) the reaction among different chemical species present in the reactor, (*iii*) the cell-dependent contribution to the concentration of such species. Thus, the changes in the Aca concentration is given by

$$\frac{\mathrm{d}\,[\mathrm{Aca}]}{\mathrm{d}t} = k_0\,\left([\mathrm{Aca}]_0 - [\mathrm{Aca}]\right) - k\,[\mathrm{CN}^-][\mathrm{Aca}] + v_{\mathrm{cells}}$$

where k_0 is the specific flow rate of the reactor, $[\mathrm{Aca}]_0$ is the mixed flow Aca concentration, k is the second-order rate constant describing the kinetics of the reaction between cyanide and Aca, and v_{cells} is the cellular Aca production rate. The relaxation parameter τ in the model corresponds to the rate of extracellular Aca removal, $\tau = k_0 + k\,[\mathrm{CN}^-]$.

All these parameters can be estimated separately, with the exception of k, which we determine from the steady-state Aca concentration $[\mathrm{Aca}]_{\mathrm{ss}}$ in the presence of oscillating yeast cells. In doing this, we approximate the concentrations to the steady state around which they oscillate. This is not expected to significantly affect the result, since the amplitude of the oscillations is small compared to their average. For the steady state we get:

$$\tau = k_0 + k[\mathrm{CN}^-]_{\mathrm{ss}} = k_0 + \frac{v_{\mathrm{cells}} + k_0\,([\mathrm{Aca}]_0 - [\mathrm{Aca}]_{\mathrm{ss}})}{[\mathrm{Aca}]_{\mathrm{ss}}}. \qquad \textbf{(S7)}$$

The parameters of our open-flow reactor are $k_0 = 0.062$ min^{-1} and $[\mathrm{Aca}]_0 = 0.75$ mM. From ref. (3) and the correction given on p. 27 in ref. (9) we estimate $[\mathrm{Aca}]_{\mathrm{ss}} = 20\ \mu$M. At a cell density of dw= 16 mg/ml, the Aca production is estimated as $v_{\mathrm{cells}} = 100\ \mu$M/min (10). By substituting these values in Eq. **S7**, one obtains $\tau = 7.3$ min^{-1}. This is in reasonable agreement with the value of $\tau = 9.9$ min^{-1}, which we obtain by fitting the reduced equation (Eq. **2**) to the experimental data.

[1] Richard P, Teusink B, Hemker MB, van Dam K, Westerhoff HV (1996) *Yeast* **12**: 731–740.

[2] Pikovsky A, Rosenblum M, Kurths, J (2001) *Synchronization: A Universal Concept in Nonlinear Science* (Cambridge Univ Press, New York).

[3] Richard P, Bakker BM, Teusink B, van Dam K, Westerhoff HV (1996) *Eur J Biochem* **235**: 238–241.

[4] Crank J (1970) *The Mathematics of Diffusion* (Oxford University Press, USA).

[5] Kuramoto Y (1975) in *Lecture Notes in Physics* (Springer, New York) Vol 39, pp 420–422.

[6] Danø S, Sørensen PG, Hynne F (1999) *Nature* **402**: 320–322.

[7] Danø S, Hynne F, De Monte S, d'Ovidio F, Sørensen PG, Westerhoff HV (2001) *Faraday Discuss* **120**: 261–276.

[8] Kuznetsov Y (1998) *Elements of Applied Bifurcation Theory* (Springer-Verlag, New York), 2nd Ed.

[9] Teusink B (1999) PhD thesis (University of Amsterdam, Amsterdam).

[10] Hynne F, Danø S, Sørensen PG (2001) *Biophys Chem* **94**: 121–163.